Elinvo (Electronics, Informatics, and Vocational Education)
Vol 9, No.2, 2024, pp. 331-347
ISSN 2580-6424 (printed) | ISSN 2477-2399 (online)

Implementation of 48V/350W BLDC Motor Speed Control With PID Method Using Microcontroller-Based Sensorless Techniques

Nurizka Fitra Maula[1], Sofyan Muhammad Ilman[1*], Sofian Yahya[1]

[1]Polytechnic State of Bandung, Bandung, Indonesia

Article Info

Article history:
Received August 19, 2024
Revised September 25, 2024
Accepted November 18, 2024

Keywords:
BLDC; sensorless; PID

Abstract

A brushless direct current (BLDC) motor is widely used in automotive and industrial applications due to its low noise and high performance. However, traditional BLDC motor control relies on Hall-effect sensors, which increase costs, enlarge motor dimensions, and risk errors from sensor failures. This research focuses on implementing a sensorless control system for a 350W, 48V BLDC motor. The goal is to achieve stable operation at a set speed of 250 rpm, with a steady-state error ≤3%, under varying loads from 0 Nm to 2.7 Nm. Using the Ziegler-Nichols PID tuning method, the study was conducted in the Electrical Machinery Laboratory at Bandung State Polytechnic. The results show that the sensorless control system effectively maintains setpoint speeds of 90 rpm, 120 rpm, 200 rpm, and 250 rpm. At 250 rpm, the system achieved an average steady-state error of 2.44% using PID parameters Kp = 3.13, Ki = 8.69, and Kd = 0.25. The motor's output power ranged from 136.88W at minimum load to 297.92W at maximum load, demonstrating improved efficiency and system performance.

Corresponding Author:
Email: sofyan.muhammad@polban.ac.id

INTRODUCTION

Recently, DC motors have been widely used in the industrial field because they have better performance, high power density, and lower noise than other motors. A study also shows the potential of using BLDC motors, especially in transportation, making BLDC motors a great opportunity in the industrial world [1]. The BLDC motor is driven using a PWM signal with a six-step commutation based on the hall-effect sensor reading in its drive system [2]. However, as a result of multiple failures in hall-effect sensor readings [3], Several researchers have conducted studies and research on sensorless DC motor control using various methods. They aim to create a reliable and efficient DC motor sensorless control system, especially for BLDC motors. These systems are known for their fast response, low overshoot and error, and good settling time, ensuring a stable and dependable system.

Each of these researchers has brought unique contributions to the field, advancing our understanding of sensorless DC motor control[4], A simulation of induction motor control was carried out. The results show that using the FT-PID combined method can reduce the ripple value in torque and provide a better response in all speed ranges compared to ordinary FLC. The simulation of induction motor control illustrates that the same method can be used in DC motor control. Furthermore, research on sensorless control of DC motor speed was carried out using the same EKF-based fuzzy method studied by R. P. Tripathi et al [5] This study showed a rise time value of 0.03543s, an error of ±3% with an average error of 1.5%, and an overshoot value of 17%. Similar research based on PID control was also conducted and showed optimal performance, the same as the previous research in [6]-[10].

Furthermore, there is research on the comparison of sensorless control of two types of fuzzy methods conducted by C. Buyukyildiz and I. Saritas [11] with a settling time of ±32ms at 3000 rpm and simulation of sensorless control of DC motor with ANFIS method based on Artificial Bee Colony (ABC) by S. S. Selva Pradeep and M. Marsaline Beno [12] Good results were obtained by settling time value ±0.034s, overshoot ≈0%, and steady-state error ranging from 0.006%—0.077%. These three studies almost all show the same results, namely that control with fuzzy and PID methods have their respective advantages in terms of fast response time, low overshoot, low steady-state error, and better settling time improvement.

The four studies also show that combining a method with other methods can provide a comparison. K. Sreeram [13] His research shows that fuzzy logic control can compete with PID control, so combining these two methods will improve control performance on BLDC motors, meanwhile, in a study conducted by A. Lotfy et al. [14], The researchers concluded that fuzzy logic optimized with improved FPGA has advantages in the value of rise time and low overshoot compared to ordinary fuzzy logic methods. Research conducted by D. Somwanshi et al. also reinforces this conclusion[15] The fuzzy method combined with the PID method can produce quite good output even though it is still in the simulation stage using LabView. S. Sattu et al. researched sensorless control of PMBLDC (Permanent Magnet Brushless DC) motors [16]. Using MATLAB simulation with the FLC-PI method shows efficiency and performance in controlling motor speed. This research compares FLC without PI with FLC-PI. The use of the PI method in this simulation gives good results. However, this study still has areas for improvement. To achieve better efficiency, the researcher proposes further research to add a current controller to keep it stable. This is expected to increase the stability of the starting current, reduce current waves, and increase the efficiency of the starting torque in the PMBLDC motor. In addition, further research can be expected in the form of hardware. In contrast to the research of S. Sattu et al., the research conducted by A. Salmaninejad and R. V. Mayorga [17] The DC motor is a BDCM (Brushed DC Motor) with the PID-ANFIS method and is connected to an isolated load. The research was conducted using MATLAB simulation. The results show that ANFIS can reduce the speed deviation on the BDCM shaft to a value of <2%. However, this method can only be applied by combining it with PID. Thus, the central axis in the control method remains in the presence of PI or PID methods.

Research using BDCM was also conducted by H. Qu et al [18], This research combines the Fuzzy-PID method with improved state observer-based and simulated with MATLAB. In this experiment, the researchers concluded that the observation (observer) carried out based on line voltage and line current parameters, with improved state observer-based researchers can improve stability in the observation of the control system. Thus, the control system becomes more stable and produces appropriate output with an error value of ±0.8% at 300 rpm with an overshoot value of almost 0%. The researcher also proposed that further research can be implemented in hardware. A fuzzy control method using Equal Area Creation (EAC) was carried out by U. K. Soni and R. K. Tripathi [19]. They are using a computer-tuned NI-PCI-6221 controller. The EAC-based commutation error correction and fuzzy-based EMF phase delay compensation strategies have improved sensorless control performance, especially at high speeds. The performance runs under several conditions, namely starting, steady state commutation, dynamic load change, and sudden reference speed change. The system also has fairly high efficiency, although the response in the method with PID control could be better. For example, it can reduce the start-up time by 10ms at 45V and 37ms at 6V start-up. In addition, this method has the highest efficiency of ±93% at 52% rated speed for 11250 rpm and an efficiency of ±85.3% at 100% rated speed. BLDC motor drive system using real-time permanent magnet flux monitoring was also conducted by Iepure et al [20] although speed control was not directly applied in this study.

In addition to testing the speed control of BLDC motors, researchers also test and analyze the performance of BLDC motors in a simulation [21] it also improves the power factor, reduces total harmonic distortion, and corrects commutation and phase deviation in BLDC motors, as in [22]-[23], [24]. Based on the research that has been done above, some books and research on BLDC motor theory

[25]-[27], and also several books on the theory of BLDC motor speed control systems, as in [28]-[29], [30]. An implementation of sensorless control for 48V/350W BLDC motor with PID method will be carried out to observe the output of sensorless 48V/350W BLDC motor speed control.

In previous studies, most research was only done through software simulation and not in the form of hardware implementation. In addition, research on the analysis of BLDC motor performance has been carried out through simulation and proven to have optimal results. Therefore, this research is carried out to realize the research in the form of previous simulations and optimize the system based on the research that has been done. This study aims to obtain the results of controlling a 48V/350W BLDC motor using a sensorless technique to follow the setpoint value at speeds of 90 rpm, 120 rpm, 200 rpm, and 250 rpm. The sensorless technique in BLDC motor control eliminates the need for physical position sensors, such as Hall-effect sensors, by relying on the back-electromotive force (back-EMF) generated by the motor windings. This back-EMF is used to estimate the rotor's position, allowing the system to maintain synchronization without the need for physical sensors.

In summary, this research aims to develop a sensorless BLDC motor control system using back-EMF detection to eliminate the need for physical sensors. By optimizing the control system, we hope to achieve stable performance under various load conditions, contributing to more efficient motor designs for industrial applications. Thus, this control system aims to maintain the BLDC motor speed with an average value of steady-state error ≤3% at 250 rpm for loads varying from 0Nm - 2.7Nm. This control will use the PID method based on the Arduino Mega 2560 microcontroller.

METHODS

The research method used is the experimental method. According to Sereyrath Em in his journal, experimental research plays a vital role in scientific exploration, allowing researchers to determine causal links and enhance understanding. To ensure research is impactful, it is essential to maintain methodological rigor and mitigate threats to validity. As experimental methods continue to develop, researchers must uphold high standards to contribute significantly to their disciplines.

This experimental approach starts with creating a comprehensive system block diagram that outlines the overall architecture of the project. This is followed by designing a BLDC motor driver to control the motor effectively. The next step involves developing the necessary software that implements control algorithms and processes feedback data. After the software design, data analysis is conducted to evaluate system performance and identify any areas for improvement. Subsequently, the system realization phase occurs, where all components are assembled and integrated into a functioning setup. After that, thorough testing is carried out to ensure the system operates as intended, and results and conclusions will be obtained to assess the overall effectiveness of the approach.

Block Diagram of The System

The block diagram of the sensorless control system of the 48V/350W BLDC motor is shown in Figure . In this control system, the Arduino Mega 2560 microcontroller serves as the central controller, orchestrating the various components involved in the operation of the 48V/350W Brushless DC (BLDC) motor. The Arduino is responsible for processing sensor feedback, executing control algorithms, and managing the overall functionality of the motor drive system. The BLDC motor operates as the actuator in this setup, converting electrical energy into mechanical energy to perform work.

To effectively control the BLDC motor, the system utilizes the back-electromotive force (back-EMF) generated within the motor windings. This back-EMF acts as a feedback signal that is crucial for determining the rotor position and estimating the speed of the motor. By analyzing the back-EMF, the control system can make informed decisions about the timing of commutation, which is essential for maintaining smooth motor operation.

ISSN 2580-6424 (printed) | ISSN 2477-2399 (online)

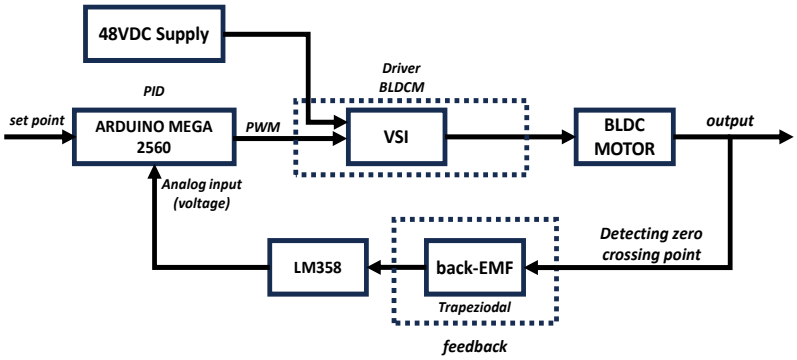

Figure 1. Block Diagram of The System

As illustrated in Figure 1, the BLDC motor drive system employs a Voltage Source Inverter (VSI) circuit configuration. The primary function of the VSI is to convert a direct current (DC) power source into a three-phase alternating current (AC) output, which is required to drive the BLDC motor. This conversion is critical because BLDC motors are designed to operate on three-phase AC power. Within the VSI circuit, MOSFETs (Metal-Oxide-Semiconductor Field-Effect Transistors) are utilized as power switches. These MOSFETs play a key role in generating the required three-phase AC voltage through a technique known as Pulse Width Modulation (PWM). PWM allows for precise control over the voltage and current supplied to the motor, thereby regulating its speed and torque output efficiently.

A critical aspect of BLDC motor operation is determining the correct commutation sequence. This sequence ensures that the magnetic field produced in the stator windings interacts optimally with the rotor magnets, allowing the motor to rotate effectively. The system relies heavily on accurate sensing of the back-EMF generated in the motor windings to achieve optimal commutation timing. Back-EMF is an induced voltage that arises when the motor windings move through a magnetic field. To detect the zero-crossing point of the back-EMF—an essential factor for establishing precise commutation timing—the system incorporates an LM358 operational amplifier. The LM358 amplifies and processes the back-EMF signal from the motor windings. The LM358 operational amplifier was selected for back-EMF detection due to its low cost, dual-output configuration, and ability to operate from a single power supply. Its stability over a wide range of temperatures ensures reliable performance in the motor control system. The LM358 is ideal for amplifying the low-level back-EMF signals generated by the motor windings, allowing for precise zero-crossing detection necessary for accurate sensorless commutation.

The zero-crossing detection method involves monitoring the point at which the back-EMF voltage crosses zero volts. When the winding back-EMF crosses zero, it indicates that it is the right moment to switch the commutation sequence to the next phase. This ensures that the VSI switches are timed appropriately to maintain rotor rotation and optimize motor performance. By accurately detecting the zero-crossing points of the back-EMF, the control system can precisely synchronize commutation with the rotor position, leading to smooth and efficient motor operation.

Additionally, the sequential turnover time of the BLDC motor rotation is used as a reference to determine the duration of one complete rotation cycle. This time is then converted into a speed calculation, which provides feedback to the Arduino. This calculated speed is essential for adjusting and maintaining the motor's performance according to the predetermined setpoint. By continuously processing this feedback, the control system can effectively manage the speed of the 48V/350W BLDC motor, ensuring it operates at the desired efficiency and responsiveness.

BLDC Motor Driver Design

In Figure 2 below, the 48V/350W Brushless DC (BLDC) motor control system is designed based on the previously established system block diagram. This design encompasses several main components

in the BLDC motor driver, including the IRFP150N power MOSFET and IR2103 IC as the gate driver, which are critical for efficient power management and control. In addition, several supporting components are integrated according to the specifications of the 48V/350W BLDC motor control system to ensure that all operational requirements for the sensorless driver are met. These components may include resistors, capacitors, and inductors that help stabilize the circuit and minimize electrical noise. This BLDC motor driver design incorporates multiple subsystems, including a microcontroller for processing inputs and controlling operations, a DC-to-DC buck-converter module to regulate voltage levels, a BLDC motor driver circuit for interfacing with the motor, and a comparator circuit for reading back-EMF voltage feedback, which is essential for accurate rotor position sensing and effective motor control.

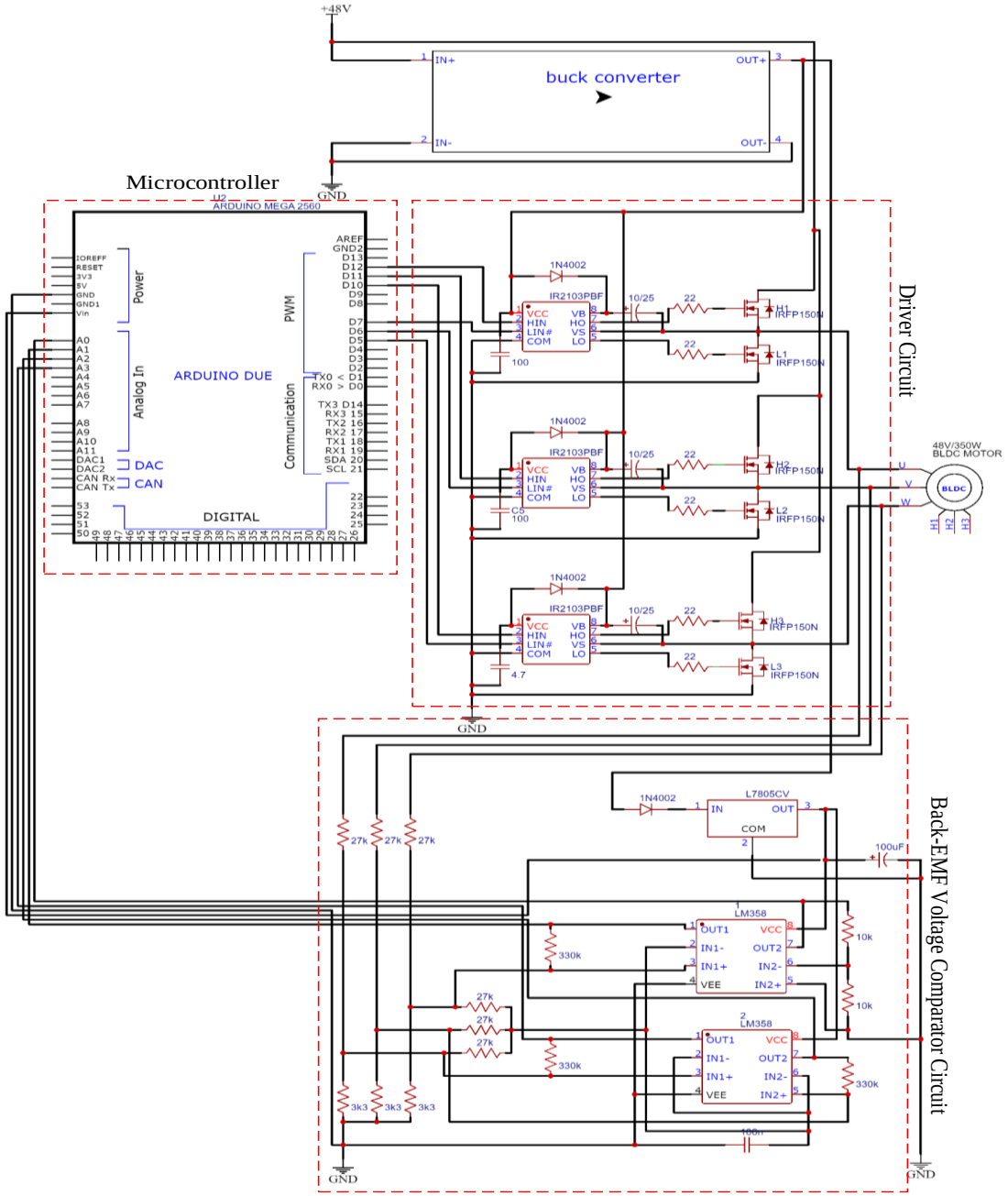

Figure 2. Overall Design of BLDC Motor Control System

The selection of the main components in the BLDC motor driver is based on several parameters. The buck converter module was chosen because it reduces the voltage from 48V to 12V for the supply of the IR2103 driver IC with an input voltage range of 10V-20V. This buck converter module can reduce

from 0V-80V supply voltage to 0V-20V output voltage. IRFP150N MOSFET performs a six-step commutation on a 48V/350W direct current brushless motor for the power switching device. The IRFP150N MOSFET was selected for its high voltage and current ratings (100V and 42A, respectively), which are well-suited for handling the 48V/350W BLDC motor's power requirements. Additionally, its low Rds(on) value minimizes power losses during switching, making it highly efficient for high-power motor control applications. This MOSFET is also known for its fast switching speed, ensuring precise commutation timing in the motor control system. Based on Equation (1), the IRFP150N MOSFET can be selected.

$$V_{DS} \times I_D \geq 350W \quad \text{.....(1)}$$

The diode in the driver circuit uses the 1N4002 type with the ability to rectify the voltage in the circuit to reach a value of 100V with a peak current of 30A. This value is by the provisions because the supply voltage used is 48V. Then, an IC component is required to drive the BLDC motor. IR2103 IC component was chosen because it can operate up to a voltage of +600V in the bootstrap circuit with a large VCC voltage ranging from 10V-20V and by the voltage output of the buck converter module. IC IR2103 also supports BLDC motor driving systems with high and low inputs for BLDC motor phase switching. To support how IR2103 IC works, the bootstrap configuration is required in the circuit. Hence, some components need to be chosen well so the system will work properly. The components needed are a diode, capacitor, and resistor. The bootstrap capacitor used is based on Equation (2).

$$C_{boot} \geq \frac{I_{load} \times t_{on}}{\Delta V_{boot}} \quad \text{.....(2)}$$

Based on the equation, the value of the capacitor that is required in this bootstrap configuration must be higher than 0,918μF. The calculation results show that the capacitor value for the bootstrap used is 10μF/25V per the provisions. Meanwhile, the diode in this bootstrap circuit uses the 1N4002 type. Then, the next step is calculating the resistor value for a bootstrap circuit. The calculation of this resistor is based on the output current of the IR2103 IC and its output voltage and a 220Ω resistor is selected according to Equation (3) below.

$$R_{boot} \geq \frac{12V}{0.27A} \quad \text{.....(3)}$$

Software Design

The software design is divided into two parts, namely the design of BLDC motor driving software and the design of PID control software. The BLDC motor driving software design involves a carefully structured algorithm that governs the operation of the BLDC motor. The process begins when the motor receives an input signal, indicating the initial rotation of the motor. After a brief delay of 20 milliseconds, the system reads the back-EMF voltage through the analog input pin, which provides critical feedback about the rotor's position. The microcontroller processes this information to accurately determine the position of the rotor, and this data is continuously updated to ensure precise control.

Based on the rotor position, the software calculates the next rotation step of the BLDC motor by identifying which phase should be activated. Once this determination is made, the corresponding phase is energized, with the high-side phase sending a Pulse Width Modulation (PWM) signal according to the predetermined duty cycle. This PWM signal effectively controls the voltage supplied to the stator winding, allowing for optimal motor performance. Simultaneously, the low-side phase is activated to drain the voltage on the stator winding to the ground, ensuring efficient operation and preventing excessive voltage buildup. After the rotor has completed its movement to the next position, the previous driving phase is deactivated or turned off, and the process is repeated. This cyclical operation relies on continuous feedback from the read back-EMF input to maintain accurate rotor position information, enabling the motor to operate smoothly and efficiently throughout its entire range of motion.

ISSN 2580-6424 (printed) | ISSN 2477-2399 (online)

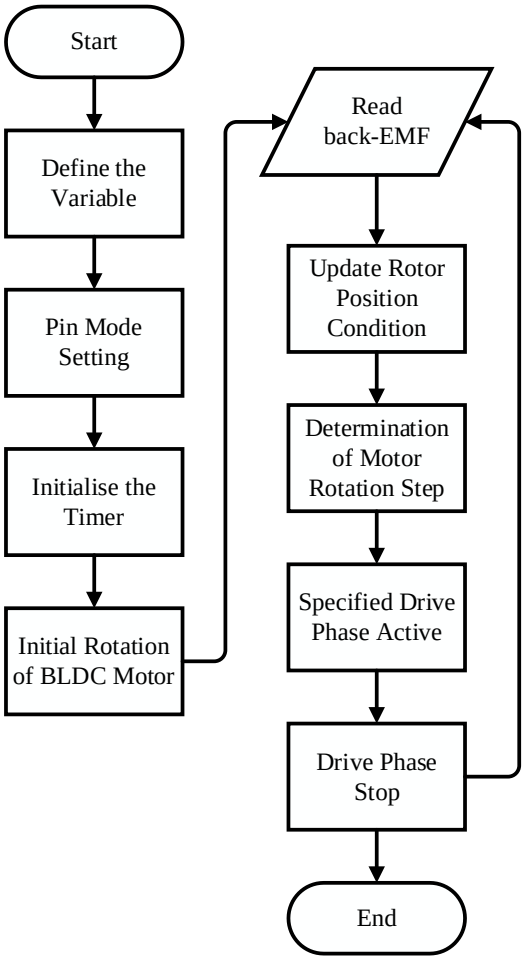

Figure 3. BLDC Motor Driving Flowchart

PID control is a widely used control strategy that combines proportional (P), integral (I), and derivative (D) actions to maintain a desired setpoint. The PID control software design controls the speed of the BLDC motor so that the motor speed can be stabilized according to the predetermined setpoint. The Figure 4 below shows the PID control flowchart.

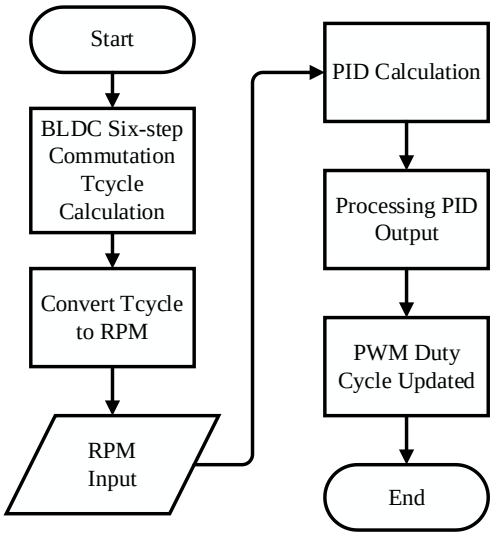

Figure 4. PID Control Flowchart

In the BLDC motor rotation, the calculation of the start-to-finish time of each of the six BLDC motor commutation steps is tcycle. This tcycle value will be obtained from how long the BLDC motor

rotates one rotation. Then the tcycle value will be converted into an rpm value by dividing the time in one minute by the time it takes to make one full rotation. This rpm value will be the setpoint according to the specified rpm value. After knowing the rpm input, the next step is calculating the PID value where the output of the PID calculation will be used to update the PWM duty cycle value.

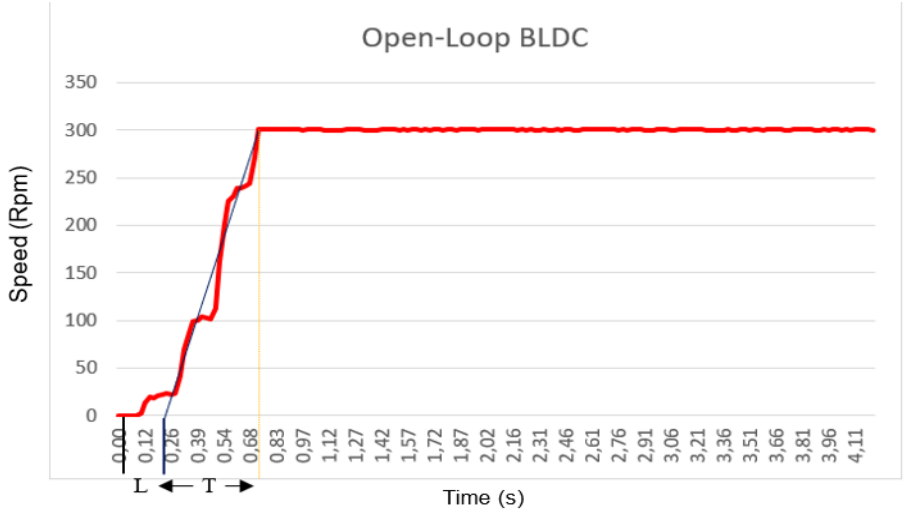

Figure 5. Open-Loop Response Graph

Based on the open valve response graph above, the following calculation is obtained:

$$L = 0.16s \quad \text{.....(4)}$$

$$T = 0.47s \quad \text{.....(5)}$$

Description:
L = Lag Time or Dead Time
T = Time Constant

After obtaining the L and T values based on the graph, the next step is to find the Kp, Ti, and Td values.

$$Kp = 1.2\ (T/L) \quad \text{.....(6)}$$

$$Ti = 2L \quad \text{.....(7)}$$

$$Td = 0.5L \quad \text{.....(8)}$$

The last step is to convert the Ti and Td values obtained into Ki and Kd values according to Equation (9) and Equation (10).

$$Ki = Kp/Ti \quad \text{.....(9)}$$

$$Kd = Kp\ x\ Td \quad \text{.....(10)}$$

After all the PID control parameters have been obtained, the following parameter values will be used in the PID control program later.

Table 1. BLDC PID Control Parameters

Parameters	Kp	Ti	Td
P	2.9375	∞	0
I	2.64375	0.533	0
PID	3.13	0.36	0.08

After calculating the initial PID parameters, the system was tested with varying loads and speeds to observe its performance. Adjustments were made based on the observed response characteristics, focusing on reducing overshoot and enhancing settling time. A loop was created to iteratively adjust the parameters and record performance metrics until the desired stability was achieved. After performing PID control calculations by the calculation of these Kp, Ti, and Td parameters. The next step is to enter the results of the PID control calculation into the Arduino IDE software and then upload it into the Arduino Mega 2560 microcontroller.

Data Analysis

The data collected from the experiments will be analyzed using statistical techniques, including descriptive statistics to summarize the data and inferential statistics to conclude. The analysis will focus on the average steady-state error, response times, and system stability under varying load conditions. Thus, to ensure the reliability of the analysis, multiple trials will be conducted for each condition, and the results will be averaged.

System Realisation

The following figure shows the realization of the BLDC motor driver on a designed PCB, including combining it with the Arduino Mega 2560 microcontroller.

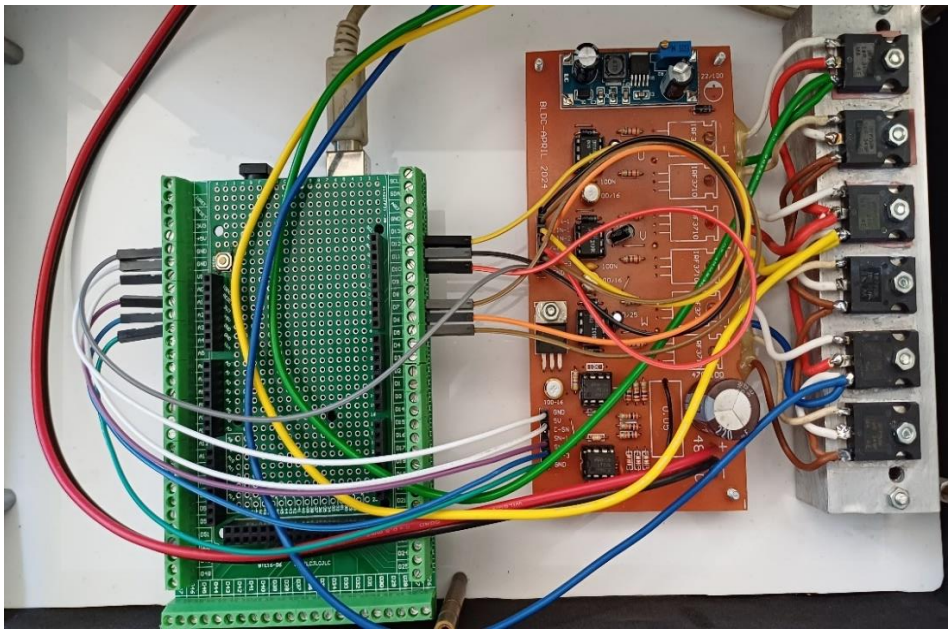

Figure 6. Realisation of 48V/350W BLDC Inverter

The BLDC motor inverter in Figure 6 above is connected to the Arduino Mega 2560 using jumper cables on each pin. All high-input and low-input pins are connected to the digital pins on the Arduino, while the back-EMF voltage feedback is connected to the analog pins of the Arduino for each pin. In addition, the Arduino is also connected to a PC via a serial cable for communication.

ISSN 2580-6424 (printed) | ISSN 2477-2399 (online)

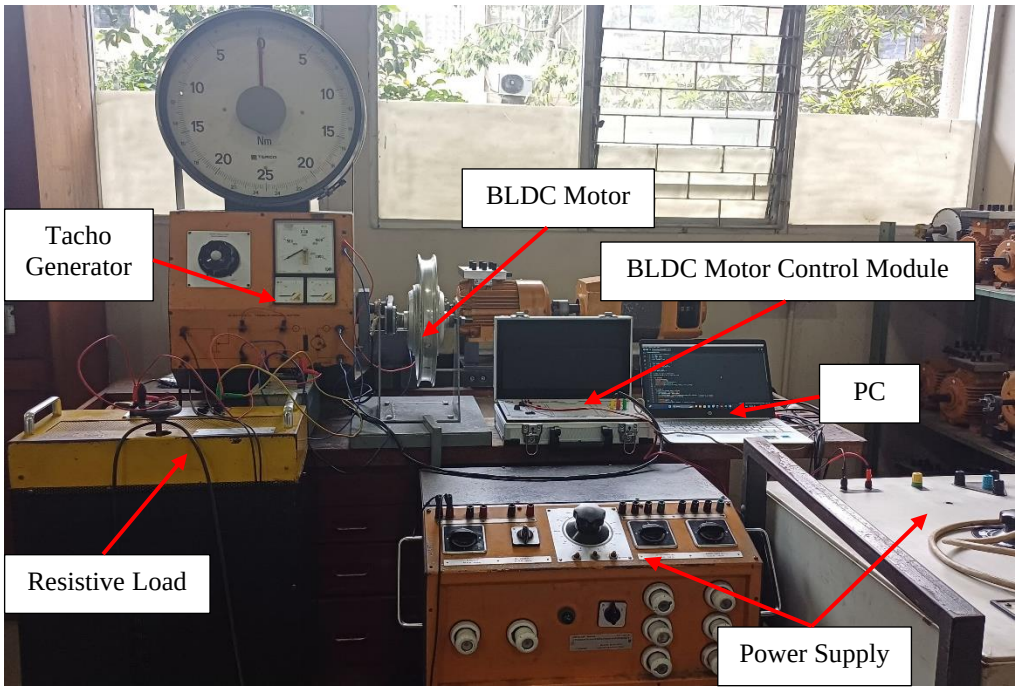

Figure 7. System Realisation

This 48V/350W BLDC motor control system uses a 0-600V 10A DC power supply. There is a power supply in the middle for supplying the tacho generator. The tacho generator reads the actual speed of the BLDC motor and adds load to the generator. Meanwhile, PC is used to set the setpoint value to determine the speed of the BLDC motor. In addition, in the realization of this system, the 48V/350W BLDC motor is connected to a tacho generator with an additional resistive load using a v-belt to represent the loading on the BLDC motor.

In conclusion, the experimental setup involves using an Arduino Mega 2560 to control the BLDC motor with a sensorless approach. Key components such as the back-EMF detection system and the MOSFET-based inverter design ensure precise commutation and speed control under varying conditions.

RESULT AND DISCUSSION

The test results are divided into several sub-sections to determine several parameters of the BLDC motor. To validate the experimental results, the motor speed obtained from the tacho generator will be compared to the expected setpoint values. A statistical analysis will be conducted to determine the average steady-state error and response times under various load conditions. The data will be recorded over multiple trials to assess the consistency and reliability of the performance metrics. Then, the experimental outcomes will be considered valid if the average steady-state error remains within the target limit of ±3% for the specified load range (0Nm to 2.7Nm). Additionally, the system's response time will be analyzed to ensure it meets the design specifications for speed control.

Response Results of PID-Controlled BLDC Motor with Changing Setpoints

As described in the Methods, the MOSFETs control the switching operation, and back-EMF is used for detecting rotor position. This test begins by observing the BLDC motor speed response to setpoint values that change from 90 rpm to 250 rpm. It aims to determine the performance of the PID control.

ISSN 2580-6424 (printed) | ISSN 2477-2399 (online)

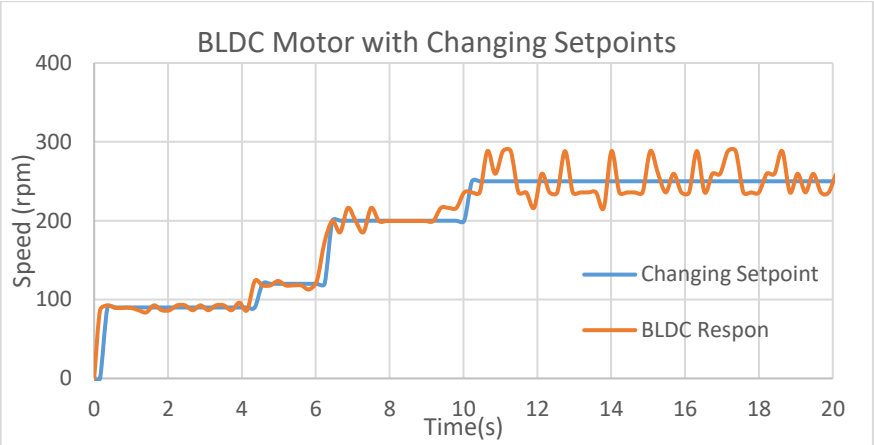

Figure 8. Speed Control Response when Setpoint Changes

Based on Figure 8 above, the motor is given an initial setpoint value of 90 rpm and shows a good response with an error value of <2%. After 4s passed, the setpoint value was increased to 120 rpm and still showed a not-too-large amount of error. When the setpoint value is increased to 200 rpm, it can be seen that the motor speed fluctuates during the rise time and experiences overshoot before finally the motor speed stabilizes. However, when the setpoint value is increased to 250 rpm, the overshoot value looks quite high and the motor speed fluctuates continuously, so the steady state error value is quite large at the 250 rpm setpoint. Fluctuations in BLDC motor speed readings can occur due to several things, namely high noise so that the back-EMF signal reading is unstable, control algorithms that are still not perfectly tuned, unstable supply voltage, and temperature problems due to high power dissipation at high speeds that affect the performance of the driver so that the speed reading on the serial monitor becomes less stable. After observing the BLDC motor speed response to the setpoint, the test continued by gradually observing the duty cycle value at each BLDC motor speed setpoint. The following table shows the PWM duty cycle value, speed, and speed setpoint.

Table 2. Duty Cycle Response to Motor Speed Setpoint

Speed (rpm)	Duty cycle	Speed Setpoint (rpm)	PWM Frequency (kHz)
92,68	78	90	62
102,44	86	100	62
110,67	95	110	62
117,95	102	120	62
127,45	110	130	62
141,32	119	140	62
155,10	127	150	62
161,75	136	160	62
173,98	144	170	62
181,24	153	180	62
190,55	161	190	62
199,62	169	200	62
208,57	177	210	62
217,95	185	220	62
228,37	193	230	62
238,55	202	240	62
259,50	214	250	62

Then the test continues by testing the system in an open-loop state, tests were conducted using the open-loop method on the system to determine the response of the BLDC motor. The test was conducted by setting the setpoint of the BLDC motor speed at 300 rpm with a duty cycle value of 254 from 255 and the PWM frequency was at a constant condition with a PWM frequency value of 62kHz. The following are the results of the BLDC motor open-loop test at a setpoint of 300 rpm.

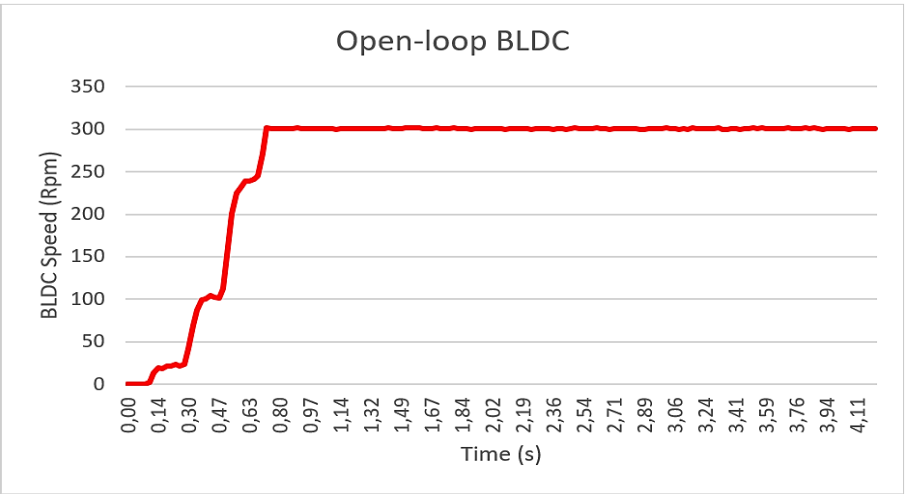

Figure 9. BLDC Motor Open-loop Response Graph

Based on Figure 9 above, it can be seen that the motor response is fast enough to reach the predetermined setpoint value. The BLDC motor speed can reach the setpoint value in approximately 0.73s from the initial time of response increase in the range of 0.08s. After observing the BLDC motor speed response in open-loop testing, the test continued by observing the output power of the BLDC motor in stages over the BLDC motor speed range of 90 rpm to 250 rpm. This output power value refers to the per-turn of the BLDC motor without load. The current measured in each phase is constant in the range of 1.7A, so the output power of the BLDC motor in this no-load condition is not so large. The following graph shows the output power of the BLDC motor.

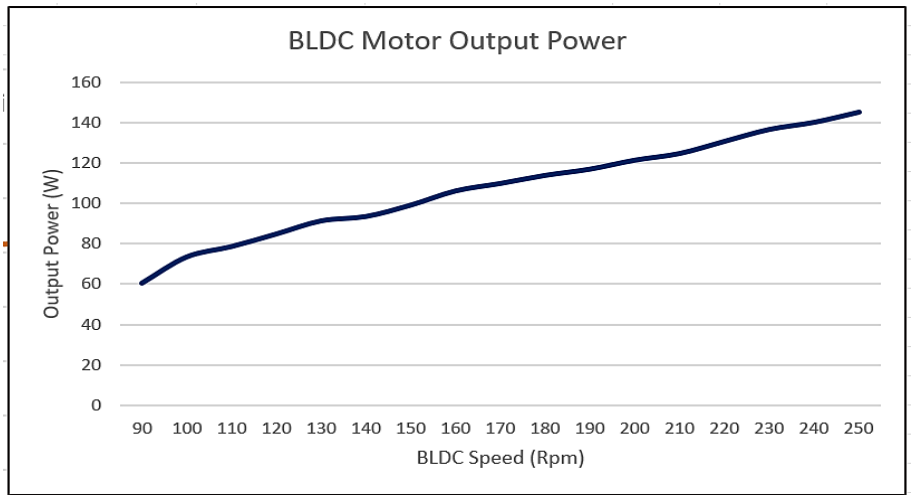

Figure 10. Open-loop BLDC Motor Output Power Chart

After testing the speed response of the open-loop BLDC motor without load and observing the output power of the BLDC motor in the speed range of 90 rpm to 250 rpm, the next step is to test the BLDC motor with a load without control. The test is carried out by connecting the BLDC motor with a load on the tacho generator so that it can be seen how much the speed drop in the BLDC motor is based on the given load range. This test was carried out by giving a setpoint to the BLDC motor at a speed of

300 rpm with a duty cycle value at 254 from 255 and a constant PWM frequency value at 62kHz. The load given to the BLDC motor ranges from 0-2.7Nm with a load ratio in each test of 0.3Nm.

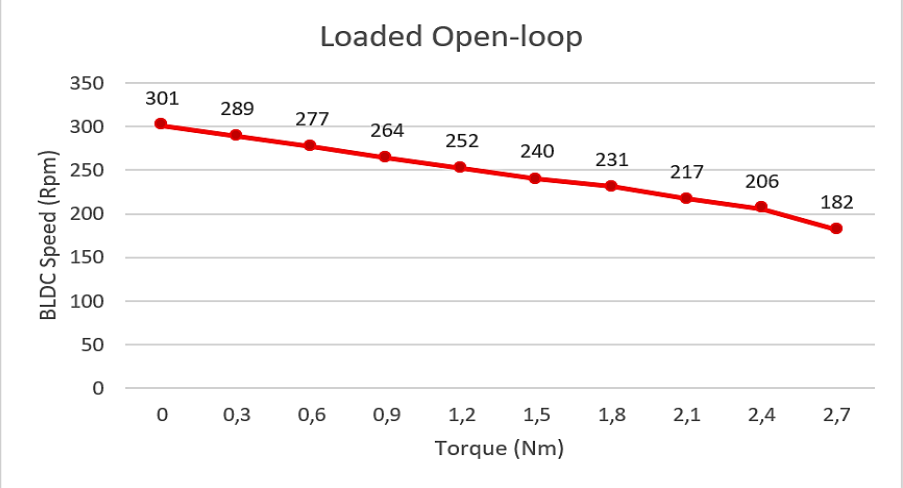

Figure 11. Response Graph of Open-loop Loaded BLDC Motor

In Figure 11 above, it can be seen that increasing torque affects the rotation speed of the BLDC motor in the open lup condition. The speed of the BLDC motor will continue to decrease as the torque increases based on the load given. This decrease occurs until the motor is given a load worth 2.7Nm and results in a decrease in motor speed until it reaches 182 rpm. The motor does not maintain speed in this condition because PID control has not been applied to the system.

Response Results of a PID-Controlled BLDC Motor with a Fixed Setpoint

This test is conducted to determine the performance of PID control with a fixed setpoint, which is 250 rpm. Figure 13 shows the test results of PID control with a fixed setpoint.

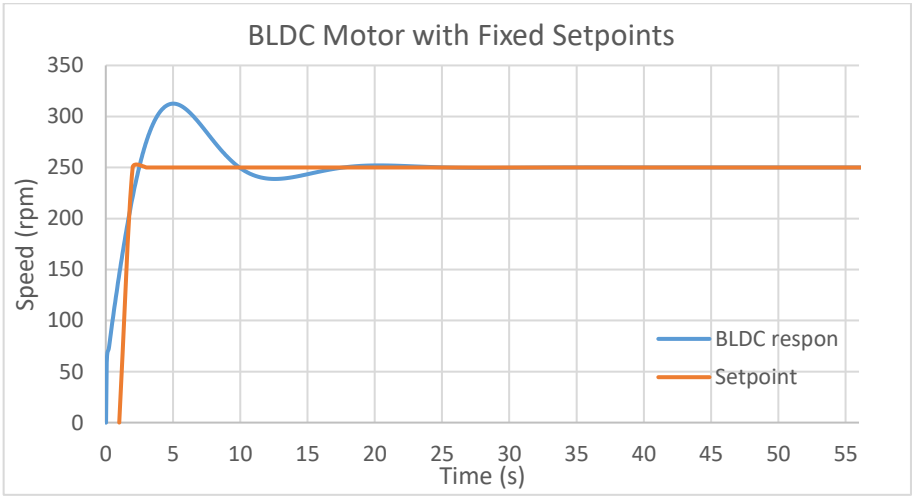

Figure 12. Speed Control Response when The Setpoint is Fixed

Figure 12 above shows the PID control response with the setpoint fixed at 250 rpm. In this test, there is an overshoot at the beginning of the BLDC motor rotation at 3 to 8 seconds with a maximum overshoot of 16.6%. Next, the loaded closed-loop test was carried out by connecting the resistive load on the tacho generator with the BLDC motor through the v-belt intermediary. In addition, in this test, a PID control system was applied to maintain the stability of the BLDC motor speed. The first test was conducted by observing the output power of the BLDC motor under load conditions of 0-2.7Nm at a setpoint of 250 rpm. In this test, the output power of the BLDC motor is also measured when given a

load. However, in this test, the current in each phase of the motor changes as the load received by the BLDC motor increases. The following graph shows the output power of the BLDC motor when loaded.

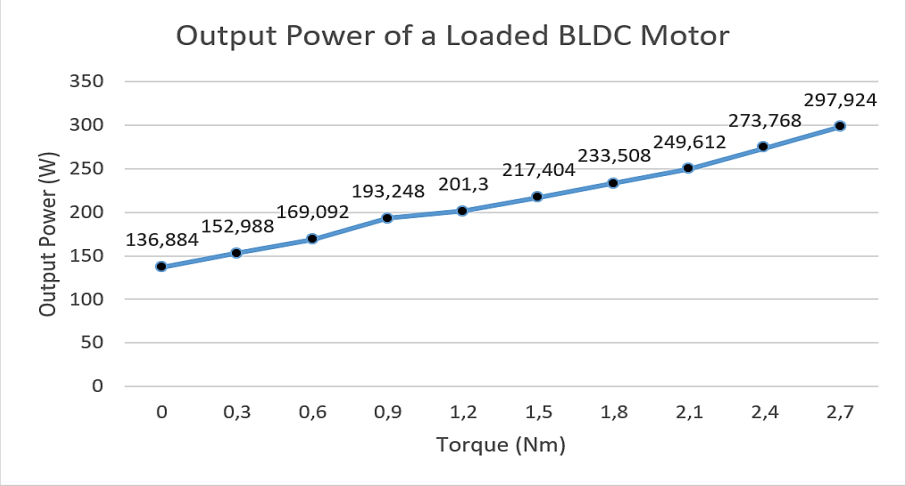

Figure 13. Graph of Output Power of a Loaded BLDC Motor

According to the graph above, with the increase in current as the load increases, the output power value of the BLDC motor will also increase. After observing the output power of the BLDC motor under load conditions at a setpoint of 250 rpm, the next step is to observe the results of testing the system with PID control when loaded. Tests were carried out with PID parameter values based on Ziegler Nichols 1 tuning calculations with loads varying from 0-2.7Nm. This test is carried out to maintain the stability of the BLDC motor speed at a setpoint value of 250 rpm. The results of this test can be seen in the table below.

Table 3. Loaded Closed-loop Testing Results

Speed Setpoint (rpm)	Speed in Serial Monitor (rpm)	Torque (Nm)	Speed in Tacho Generator (rpm)	Input DC Voltage (V)	Current (A)	PWM Frequency (kHz)	Duty Cycle	Error (%)
250	259	0	252	47,36	0,736	62	209	3,6
250	259	0,3	251	47,23	1,037	62	214	3,6
250	249	0,6	251	47,06	1,119	62	218	0,4
250	248	0,9	252	47,01	1,376	62	221	0,8
250	254	1,2	251	47,13	1,655	62	232	1,6
250	255	1,5	250	47,22	1,826	62	234	2
250	256	1,8	250	47,16	2,082	62	238	2,4
250	251	2,1	248	47,11	2,437	62	246	0,4
250	241	2,4	247	47,23	2,677	62	250	3,6
250	235	2,7	245	47,08	2,994	62	254	6

From Table 3, the test results were obtained in maintaining the BLDC motor speed at a setpoint of 250 rpm using PID control given a load varying from 0-2.7Nm. The motor speed begins to decrease at a load of 2.7Nm, this occurs due to the duty cycle value that has reached the maximum limit. This duty cycle value increases to keep the motor speed at the predetermined setpoint. However, because the duty cycle is already at the maximum value, the motor speed can no longer be kept constant and begins to decrease at a load of 2.7 Nm. The data in the table above shows that the BLDC motor speed error value tends to stabilize until it reaches a load of 2.7Nm with an average steady-state error value of 2.44%. This level of accuracy is generally considered acceptable for many industrial applications,

indicating that the control strategy implemented is effective. The observed steady-state error of 2.44% suggests that while the system performs satisfactorily within the designed parameters, improvements in the control algorithm may yield better accuracy. Continuous monitoring and adaptive tuning of the PID parameters can help minimize the impact of external disturbances, thereby enhancing the overall reliability of the motor control system.

To summarize, the results demonstrate that the sensorless control method successfully maintained motor speed with minimal error across a range of load conditions. Additionally, the PID tuning approach using the Ziegler-Nichols method allowed for improved performance, although further tuning could enhance system stability at higher speeds.

CONCLUSION

Our study implemented a BLDC motor speed control system using a sensorless technique based on the Arduino Mega 2560 microcontroller. The system operated at a speed setpoint value of 250 rpm, and the results align with our objectives, with an average steady-state error of 2.44%. Notably, the system could track the setpoint at a range of motor speeds, including 90 rpm, 120 rpm, 200 rpm, and 250 rpm, demonstrating its versatility and reliability. The sensorless control method developed in this research offers significant practical applications across various industries, particularly in robotics, automotive, and consumer electronics. In robotics, it enhances efficiency by enabling BLDC motors to operate without physical sensors, thereby reducing costs and improving reliability in manufacturing and assembly tasks. In addition, there are suggestions for future research. Conducting long-term performance assessments will be crucial to evaluate the system's durability and effectiveness in real-world applications. Afterward, improve the quality of tuning the MOSFET switching time so that speed readings using sensorless techniques can be more accurate. Then, all sensorless starting and commutation techniques are expected to be applied to compare the results of other starting and commutation method systems with the methods in this test.

ACKNOWLEDGMENT

The authors would like to express their gratitude to the supervisors for their guidance and support during this research, to the Polytechnic State of Bandung campus which has allowed the author to conduct research, as well as to the Power Control and Electrical Machinery Laboratory of Bandung State Polytechnic which has facilitated this research. In addition, the author would also like to thank the funders of this research and all colleagues who have helped this research.

REFERENCES

[1] M. S. R. S. M. Reza Bastari Imran Watimea, “Pertimbangan Pelanggan Terhadap Keinginan Membeli (Purchase Intention) Motor Listrik,” *JPTD*, vol. 24, no. 1, pp. 21–27, Jun. 2022, doi: 10.25104/jptd.v24i1.2097.

[2] M. R. Rusli *et al.*, “BLDC Motor Drives with A Programmable Simplified C-Block to Generate Accurate Six-Step PWM Based on STM32 Microcontroller,” *ELINVO*, vol. 7, no. 2, pp. 112–118, Jan. 2023, doi: 10.21831/elinvo.v7i2.52992.

[3] G. Scelba, G. De Donato, M. Pulvirenti, F. Giulii Capponi, and G. Scarcella, “Hall-Effect Sensor Fault Detection, Identification, and Compensation in Brushless DC Drives,” *IEEE Trans. on Ind. Applicat.*, vol. 52, no. 2, pp. 1542–1554, Mar. 2016, doi: 10.1109/TIA.2015.2506139.

[4] V. S. Virkar and S. S. Karvekar, “Luenberger observer based sensorless speed control of induction motor with Fuzzy tuned PID controller,” in *2019 International Conference on Communication and Electronics Systems (ICCES)*, Coimbatore, India: IEEE, Jul. 2019, pp. 503–508. doi: 10.1109/ICCES45898.2019.9002268.

[5] R. P. Tripathi, A. K. Singh, P. Gangwar, and R. K. Verma, “Sensorless speed control of DC motor using EKF estimator and TSK fuzzy logic controller,” *Automatika*, vol. 63, no. 2, pp. 338–348, Apr. 2022, doi: 10.1080/00051144.2022.2039990.

[6] K. Vanchinathan, K. R. Valluvan, C. Gnanavel, and C. Gokul, "Design methodology and experimental verification of intelligent speed controllers for sensorless permanent magnet BRUSHLESS DC motor: Intelligent speed controllers for electric motor," *Int Trans Electr Energ Syst*, vol. 31, no. 9, Sep. 2021, doi: 10.1002/2050-7038.12991.

[7] K. Vanchinathan and K. R. Valluvan, "A Metaheuristic Optimization Approach for Tuning of Fractional-Order PID Controller for Speed Control of Sensorless BLDC Motor," *J CIRCUIT SYST COMP*, vol. 27, no. 08, p. 1850123, Jul. 2018, doi: 10.1142/S0218126618501232.

[8] S. Usha, P. M. Dubey, R. Ramya, and M. V. Suganyadevi, "Performance enhancement of BLDC motor using PID controller," *IJPEDS*, vol. 12, no. 3, p. 1335, Sep. 2021, doi: 10.11591/ijpeds.v12.i3.pp1335-1344.

[9] K. Vanchinathan and K. R. Valluvan, "Tuning of Fractional Order Proportional Integral Derivative Controller for Speed Control of Sensorless BLDC Motor using Artificial Bee Colony Optimization Technique," in *Intelligent and Efficient Electrical Systems*, vol. 446, M. C. Bhuvaneswari and J. Saxena, Eds., in Lecture Notes in Electrical Engineering, vol. 446. , Singapore: Springer Singapore, 2018, pp. 117–127. doi: 10.1007/978-981-10-4852-4_11.

[10] P. D. S. and S. K. R., "Artificial Neural Network with Optimized FOPID for Speed Control of Sensorless BLDC Motor Drive," *Cybernetics and Systems*, pp. 1–23, Dec. 2022, doi: 10.1080/01969722.2022.2148920.

[11] C. Buyukyildiz and I. Saritas, "Sensorless Brushless DC Motor Control Using Type-2 Fuzzy Logic," *International Journal of Intelligent Systems and Applications in Engineering*.

[12] S. S. Selva Pradeep and M. Marsaline Beno, "Hybrid Sensorless Speed Control Technique for BLDC Motor Using ANFIS Automation," *Intelligent Automation & Soft Computing*, vol. 33, no. 3, pp. 1757–1770, 2022, doi: 10.32604/iasc.2022.023470.

[13] K. Sreeram, "Design of Fuzzy Logic Controller for Speed Control of Sensorless BLDC Motor Drive," in *2018 International Conference on Control, Power, Communication and Computing Technologies (ICCPCCT)*, Kannur: IEEE, Mar. 2018, pp. 18–24. doi: 10.1109/ICCPCCT.2018.8574280.

[14] A. Lotfy, M. Kaveh, M. R. Mosavi, and A. R. Rahmati, "An enhanced fuzzy controller based on improved genetic algorithm for speed control of DC motors," *Analog Integr Circ Sig Process*, vol. 105, no. 2, pp. 141–155, Nov. 2020, doi: 10.1007/s10470-020-01599-9.

[15] D. Somwanshi, M. Bundele, G. Kumar, and G. Parashar, "Comparison of Fuzzy-PID and PID Controller for Speed Control of DC Motor using LabVIEW," *Procedia Computer Science*, vol. 152, pp. 252–260, 2019, doi: 10.1016/j.procs.2019.05.019.

[16] S. Sattu, V. K. Awaar, and P. Jugge, "Speed control of robust position sensor less PMBLDC motor by Fuzzy controller," *E3S Web Conf.*, vol. 309, p. 01063, 2021, doi: 10.1051/e3sconf/202130901063.

[17] A. Salmaninejad and R. V. Mayorga, "Sensor-less Brushed DC Motor Speed Control with Intelligent Controllers," *WSEAS TRANSACTIONS ON SYSTEMS*, vol. 20, pp. 140–148, Jul. 2021, doi: 10.37394/23202.2021.20.16.

[18] H. Qu, J. Zeng, R. Sheng, and Y. Guo, "Research on Sensorless Fuzzy PID Control of BDCM based on Improved State Observer:," in *Proceedings of 5th International Conference on Vehicle, Mechanical and Electrical Engineering*, Dalian City, China: SCITEPRESS - Science and Technology Publications, 2019, pp. 416–420. doi: 10.5220/0008868704160420.

[19] U. K. Soni and R. K. Tripathi, "Sensorless control of high-speed BLDC motor using equal area criterion based precise commutation scheme with Fuzzy based phase delay compensation," *Int Trans Electr Energ Syst*, vol. 31, no. 9, Sep. 2021, doi: 10.1002/2050-7038.13001.

[20] L. I. Iepure, I. Boldea, and F. Blaabjerg, "Hybrid I-f Starting and Observer-Based Sensorless Control of Single-Phase BLDC-PM Motor Drives," *IEEE Trans. Ind. Electron.*, vol. 59, no. 9, pp. 3436–3444, Sep. 2012, doi: 10.1109/TIE.2011.2172176.

[21] M. Mahmud, S. M., A. H., A. Nurashikin, and A. K.M., "Modeling and Performance Analysis of an Adaptive PID Speed Controller for the BLDC Motor," *IJACSA*, vol. 11, no. 7, 2020, doi: 10.14569/IJACSA.2020.0110736.

[22] L. Bin *et al.*, "A novel approach to design of a power factor correction and total harmonic distortion reduction-based BLDC motor drive," *Front. Energy Res.*, vol. 10, p. 963889, Jan. 2023, doi: 10.3389/fenrg.2022.963889.

[23] Y. Li, X. Song, X. Zhou, Z. Huang, and S. Zheng, "A Sensorless Commutation Error Correction Method for High-Speed BLDC Motors Based on Phase Current Integration," *IEEE Trans. Ind. Inf.*, vol. 16, no. 1, pp. 328–338, Jan. 2020, doi: 10.1109/TII.2019.2917608.

[24] X. Zhou, Y. Zhou, C. Peng, F. Zeng, and X. Song, "Sensorless BLDC Motor Commutation Point Detection and Phase Deviation Correction Method," *IEEE Trans. Power Electron.*, vol. 34, no. 6, pp. 5880–5892, Jun. 2019, doi: 10.1109/TPEL.2018.2867615.

[25] S.-H. Kim, "Brushless direct current motors," in *Electric Motor Control*, Elsevier, 2017, pp. 389–416. doi: 10.1016/B978-0-12-812138-2.00010-6.

[26] A. Keyhani, M. N. Marwali, L. E. Higuera, G. Athalye, and G. Baumgartner, "An Integrated Virtual Learning System for the Development of Motor Drive Systems," *IEEE Power Eng. Rev.*, vol. 22, no. 1, pp. 67–68, Jan. 2002, doi: 10.1109/MPER.2002.4311675.

[27] R. F. Anugrah, "Kontrol Kecepatan Motor Brushless DC Menggunakan Six Step Comutation Dengan Kontrol PID (Propotional Integral Derivative)," J. Tek. Elektro dan Komput. TRIAC, vol. 7, no. 2, pp. 57–63, 2020, doi: 10.21107/triac.v7i2.7923.

[28] K. J. Åström and B. Wittenmark, *Adaptive control*, 2. ed. Mineola, N.Y: Dover Publ, 2008.

[29] N. S. Nise, *Control systems engineering*, Seventh edition. Hoboken, NJ: Wiley, 2015.

[30] R. C. Dorf and R. H. Bishop, *Modern control systems*, Thirteenth edition. Hoboken: Pearson, 2016